ACS APPLIED MATERIALS & INTERFACES

Research Article

www.acsami.org

Significantly Enhanced Photocatalytic Activities and Charge Separation Mechanism of Pd-Decorated ZnO–Graphene Oxide Nanocomposites

Long Zhang,[†,∥] Lianhuan Du,[†,∥] Xiang Yu,[‡] Shaozao Tan,[§] Xiang Cai,[⊥] Peihua Yang,[†] Yu Gu,[†] and Wenjie Mai*[,†]

[†]Department of Physics and Siyuan Laboratory, Jinan University, Guangzhou, Guangdong 510632, China

[‡]Analytical and Testing Center, Jinan University, Guangzhou, Guangdong 510632, China

[§]Department of Chemistry, Jinan University, Guangzhou, Guangdong 510632, China

[⊥]Department of Light Chemical Engineering, Guangdong Polytechnic, Foshan 528041, China

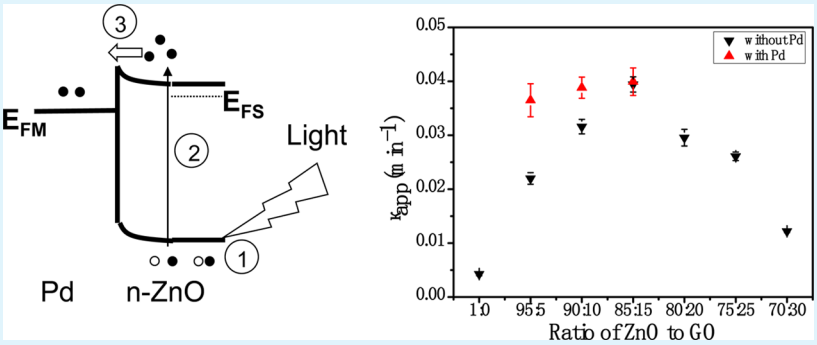

ABSTRACT: Electron–hole recombination is one of the major factors limiting the efficiency of ZnO-based photocatalysts. In this work, a 2-fold enhancement strategy was employed to suppress electron–hole recombination and boost photocatalytic efficiency. First, significantly enhanced photocatalytic activity of ZnO by introducing graphene oxide (GO) was systematically investigated. Hybrid photocatalysts with different weight ratios of ZnO to GO (from 0.95:0.05 to 0.70:0.30) were synthesized and characterized. The results indicated that when the proportion ratio of ZnO to GO reached 0.85:0.15, the as-synthesized ZnO–GO nanocomposite exhibited the maximum photocatalytic efficiency on methylene blue with an apparent rate constant κ_{app} almost 10 times faster than that of pure ZnO under UV illumination. GO was suggested to enhance the photocatalytic activity of ZnO because of its great capability in dye adsorption and charge separation. Second, Pd nanoparticles were introduced to decorate ZnO–GO to produce generally better photocatalyst ZnO–GO–Pd nanocomposites. The junction between Pd and ZnO was believed to also effectively separate the photogenerated charges due to the metal-semiconductor diode effect. These two systems of ZnO–GO and ZnO–GO–Pd nanocomposites are expected to have a broad range of applications in environmental conservation.

KEYWORDS: *ZnO, graphene oxide, photocatalytic activity, charge separation*

1. INTRODUCTION

Graphene has emerged as a novel nanocarbon material in recent research.[1−3] This kind of two-dimensional macromolecular sheet of carbon atoms material exhibits many superiorities such as a flexible structure, large specific surface area,[4] unique electronic property,[5,6] and high transparency,[7] attributed to its one atom thickness structure. Graphene oxide (GO) contains a series of reactive oxygen functional groups on the sheet surface that could be regarded as graphene functionalized by carboxylic acid, hydroxyl, and epoxide groups. Owing to these functional groups, GO solves the problem of graphene aggregating readily in solutions caused by strong van der Waals force. This makes GO a good choice for supporting metal or metal oxide particles. In addition, GO can be gained from graphite easily and sufficiently, and degree of oxidation can be controlled by adjusting reaction conditions.

The photocatalytic decomposition of organic dyes has drawn much attention due to their huge amount discharged every year from industries and households, and their great hazards on the environment. Oxide semiconductors such as titanium dioxide (TiO_2) and zinc oxide (ZnO) have been widely used for pollutant degradation due to their many advantages such as low cost, abundance, nontoxicity, physical and chemical stability, and high efficiency.[8−12] These materials are widely believed to be the most promising materials to have a practical application

Received: December 19, 2013
Accepted: February 18, 2014
Published: February 18, 2014

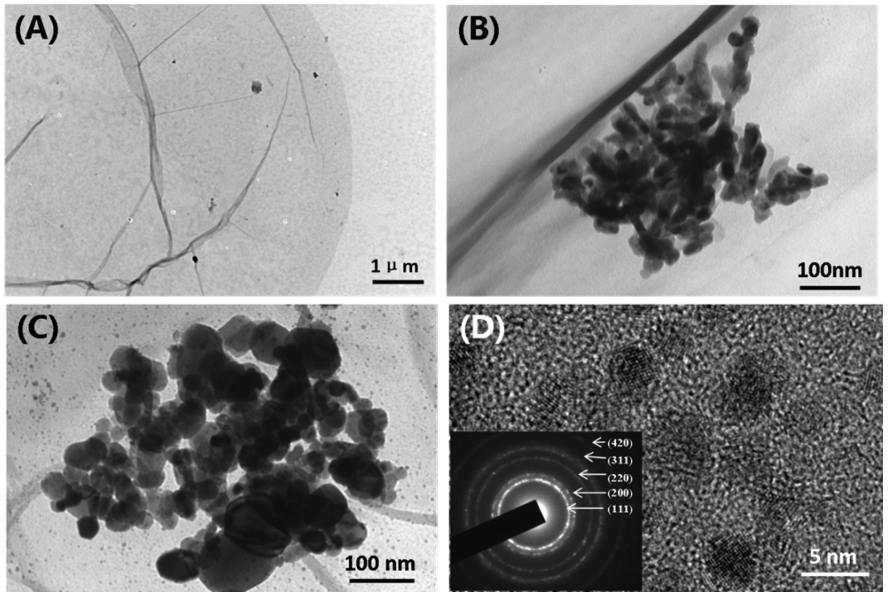

Figure 1. TEM images of (A) GO (B) ZnO−GO (C) ZnO−GO−Pd and HRTEM image of (D)Pd NPs. Inset is the corresponding electron diffraction pattern of Pd NPs shown in (D).

in reality, and one essential problem to be settled to further improve their performance is how to retard the recombination of the photogenerated electrons and holes. The recombination process usually has faster kinetics than the surface redox reactions, greatly reducing the quantum efficiency of photocatalysis. Many efforts have been reported to prevent the quick recombination of electron−hole pairs, such as using semiconductor hybrids with noble metals,[13,14] metal oxide,[15,16] and carbon materials (graphene and GO).[17−20] Jiang et al. developed a novel method to synthesize GO/TiO_2 composites as a highly efficient photocatalyst by in situ depositing TiO_2 nanoparticles on GO nanosheets via a liquid phase deposition.[21] The composites had a two-dimensional porous structure and showed a considerably larger surface area than that of pure P25 and the similarly prepared TiO_2 particles without GO. Furthermore, the GO/TiO_2 also exhibited higher rates for degrading methyl orange and reducing Cr(VI) as compared to those for pure P25. Chen et al. reported another method to fabricate high efficiency photocatalysts using GO and $TiCl_3$ as reactants via a self-assembly method.[22] It was found that either a p-type or n-type semiconductor was formed by GO in GO/TiO2 composites with different concentrations of GO in the starting solution. When GO formed a p-type semiconductor, a p/n heterojunction could be clearly observed. The concentration of GO in the starting solution also played an important role in photoelectronic and photocatalytic performance of GO/TiO_2 composites. The as-synthesized composites could decompose methyl orange under visible light irradiation efficiently. Another interesting result for TiO_2 nanorods self-assembled on GO sheets was reported by Liu et al. that one two-phase process for self-assembling TiO_2 nanorods on the whole large GO sheets were created.[23] This work provides an excellent method for assembling and stabilizing the high-quality organic soluble nanocrystals on large GO sheets. The as-synthesized photocatalysts exhibit a higher photocatalytic activity than GO−P25 and the original TiO_2 under UV light irradiation. In addition, decorating semiconductor catalysts by using noble metal nanoparticles such as Ag, Au, and Pd to improve the photocatalytic efficiency has also been reported.[24−26] Hankare et al. integrally reported a titania−alumina−zinc ferrite nanocomposite.[27] The presence of a Pd cocatalyst increases the photocatalytic activity of T40−ZF (composites having 40% of TiO_2 on $ZnFe_2O_4$ nanoparticles) and the photocatalytic activity of Pd−T40−ZF is comparable with that of T40−Al−ZF without a cocatalyst.

In this work, ZnO−GO nanocomposites and ZnO−GO−Pd nanocomposites have been systematically synthesized via a facile method. The significant enhancement of photocatalytic activities was observed, and the possible mechanism was proposed. These systems of nanocomposites are expected to have a broad range of applications in environmental conservation.

2. EXPERIMENTAL DETAILS

2.1. Materials and Reagents. All chemicals utilized in this work were analytical grade and were used as received. ZnO nanoparticles (NPs) were purchased from Aladdin Co., Ltd., China. Graphite powder (spectral pure) and methylene blue (MB, biological stain) were from Sinopharm Chemical Reagent Co., Ltd. Deionized (DI) water was prepared by Milli-Q Plus system (Millipore), and all solutions were prepared from the as-provided deionized water.

2.2. Preparation of GO and ZnO−GO. GO was obtained from natural graphite powder via a modified Hummers method, as originally developed by Kovtyukhova and colleagues.[28,29] A dialysis process was used to remove residual salts and acids completely. The as-purified GO powder was collected by centrifugation, dried in air, and further used for the preparation of ZnO−GO.

A facile one-step synthesis method was used here to acquire ZnO−GO nanocomposites. ZnO NPs and GO powders were mixed (with different weight ratios from 0.95:0.05 to 0.70:0.30) in DI water, and then the mixture was stirred energetically for 2 h to obtain ZnO−GO dispersion. The dispersion was centrifuged and dried to obtain ZnO−GO powder for further use.

ZnO−GO−Pd nanocomposite photocatalysts were synthesized via a thermal method. First, different amounts of GO (ranges from 0.05 to 0.3 g, with 0.05 g as a step size) were cast into DI water followed by ultrasonication for 10 min and subsequent stirring for 20 min, to disperse GO evenly. Second, 40 mg of polyvinyl pyrrolidone (PVP) was dissolved in a GO dispersion and the solution was heated up to 60 °C, marked as solution A. Third, 0.01 g of $PdCl_2$ was dissolved in 10 mL of KCl solution with the concentration of 5 mg/mL and then

mixed with solution A for 30 min. Two milliliters of formaldehyde was used to fabricate Pd NPs. Then ZnO NPs were mixed with aforementioned solution for 2 h. The samples were centrifuged and dried to obtain ZnO−GO−Pd nanocomposites.

The as-synthesized ZnO−GO and ZnO−GO−Pd nanocomposites were used as photocatalysts in the photocatalytic degradation experiments.

2.3. Photocatalytic Experiment. The photocatalyst (5 mg) was cast in 50 mL of an aqueous dye solution of 10 mg L^{-1} MB. The solution was first ultrasonicated for 5 min to disperse the photocatalysts evenly and then stirred in the dark for 30 min to establish an adsorption−desorption equilibrium. The test for measuring the photodegradation property was conducted under the UV illumination (wavelength: 254 nm, power: 8 W). At given time intervals under UV illumination, 5 mL of the solution was sampled and centrifuged to remove the photocatalyst completely. The solution was analyzed by Shimadzu UV-2550 PC spectrophotometer. Because the dye and catalyst were uniformly distributed in the solution, the change of volume should have negligible effect on the results.

2.4. Characterization. The morphology and diffraction pattern were recorded by a JEOL 2100F field emission transmission electron microscope (TEM). The crystalline nature of the ZnO−GO powder was investigated by a 2500v/pc X-ray diffractmeter (XRD) using Cu Kα radiation (Kα = 0.154 05 nm) at a scanning rate of 10.0°/min with a voltage of 40 kV and current of 200 mA. The absorption spectra of ZnO, GO, and ZnO−GO were recorded by Shimadzu UV-2550 PC spectrophotometer in the range of 300−800 nm. Fluorescence spectra were recorded by using a Hitachi F4600 fluorescence spectrophotometer.

3. RESULTS AND DISCUSSION

The morphology and structure of GO, ZnO−GO nanocomposite, and ZnO−GO−Pd nanocomposites were investigated by TEM and shown in Figure 1A−C, respectively. As shown in Figure 1A, the GO sheet wrinkles are clearly observed. According to Figure 1A, the GO sheet is basically flat, and the wrinkles of the GO sheet are attributed to the disruption of the planar sp^2 carbon sheets by the introduction of sp^3-hybridized carbon upon oxidation.[30] It is also observed from Figure 1C that the ZnO NPs and Pd NPs are dispersed on the GO sheet and the particle size of ZnO NPs loaded on GO sheet mostly ranges from 20 to 100 nm. Compared to Figure 1B, the ZnO NPs in Figure 1C are slightly bigger, probably because of coarsening. The extra small spots located on the GO sheet (Figure 1C) are Pd NPs. The high-resolution TEM and select area diffraction pattern of loaded Pd NPs are observed clearly in Figure 1D. It is observed that the diameter of Pd NPs distributes between 3 and 5 nm. The diffraction rings are indexed as (111), (200), (220), (311), and (420) of Pd from inside to outside.

The absorption range of light plays an important role in the photocatalysis. The absorption spectra of ZnO, GO, and ZnO−GO are shown in Figure 2A. The fluorescence spectra in Figure 2B describe the quenching process of ZnO by introducing different amounts of GO in solution. As the amount of GO increases, a clear emission quenching process is observed, indicating direct contacts and interactions between ZnO and GO. The significant decrease in fluorescence intensity reveals that there is an additional route for the transfer of charge carriers because of the interactions between the excited ZnO particles and the GO sheets. These kinds of interactions prevent the recombination of electrons and holes which are generated from UV light irradiation, prolongs the lifetime of the electron−hole pairs and, in turn, weakens the strength of the ZnO photoluminescence emission.

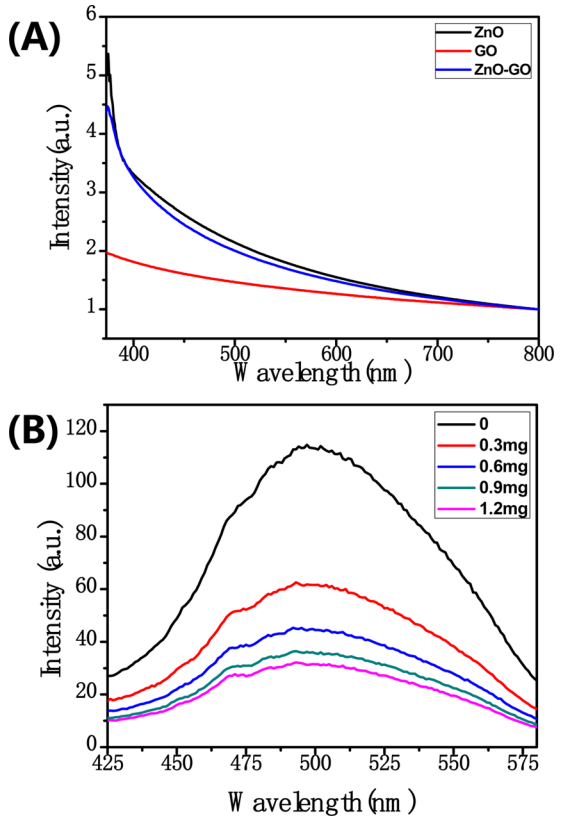

Figure 2. (A) UV−visible absorption spectra of ZnO, GO, and the resulting ZnO−GO composites. (B) Quenching process of fluorescence of ZnO with different concentrations of GO in aqueous solution.

XRD patterns of graphite, GO, ZnO, ZnO−GO (0.95:0.05 in weight ratio, same for the rest ratios), and ZnO−GO−Pd (0.85:0.15:0.005) are shown in Figure 3. For graphite, an intense crystalline peak around 26.46° is observed, which represents the characteristic peak of the (002) plane in hexagonal graphite. After oxidation, the previously mentioned

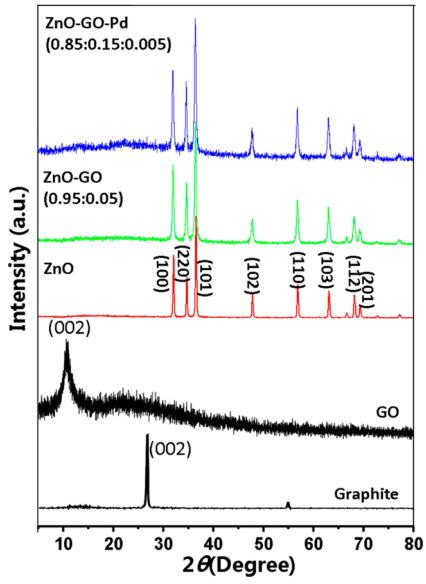

Figure 3. XRD patterns of graphite, GO, ZnO, ZnO−GO (0.95:0.05), and ZnO−GO−Pd (0.85:0.15:0.005).

dx.doi.org/10.1021/am405872r | ACS Appl. Mater. Interfaces 2014, 6, 3623−3629

peak disappears and a weak peak appears at 10.16°, which corresponds to GO's (002) plane. The oxidized and exfoliated carbon atomic layers were stacked weakly, resulting in the weak signal-to-noise ratio. This significant change of peak location indicates the great expansion of *d*-spacing due to the introduction of oxygen functionalities (such as C−OH, C−O−C, C−OOH) of GO.[31−33] The main diffraction peaks of ZnO, ZnO−GO, and ZnO−GO−Pd composites are similar to each other and correspond to hexagonal phase of ZnO, which indicates the introduction of GO and Pd does not lead to the new phase or change in preferential orientations of ZnO. Meanwhile, all peaks from three XRD patterns are narrow due to high crystallinity. No obvious diffraction peaks from Pd were observed because the quantity of Pd is too small to be detected.

An experiment has successfully been conducted in which the as-synthesized photocatalyst (the ratio of ZnO to GO is 0.85:0.15) was employed to degrade the MB solution at the UV light source (λ = 254 nm). Figure 4A illustrates that the

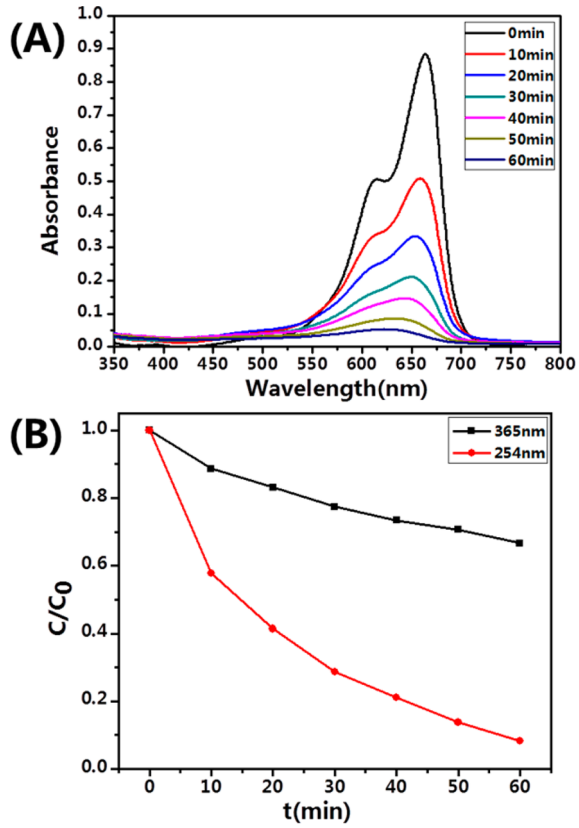

Figure 4. (A) UV−visible spectra of MB solution with ZnO−GO (0.85:0.15) as photocatalyst under UV illumination of 254 nm at different time. (B) Comparison of photodegradation processes of photocatalysts ZnO−GO (0.85:0.15) on MB under UV lights of different wavelengths.

absorption spectra revealed the process of the degradation of the MB dye after UV light irradiation. With the evolution of the degradation process, the peak values of the absorption spectra decreased gradually, which indicated the concentration of the dye solution decreased. It could be observed that the characteristic peak of the MB dye centered at 644 nm. As the description in Figure 4B indicates, a comparison about photodegradation has been made at different wavelengths with the same photocatalyst (ZnO:GO = 0.85:0.15). At λ = 365 nm, the rate of the degradation of the MB solution was lower than at λ = 254 nm. Also, the concentration of MB decreased to nearly 0.07% after irradiating for 60 min at λ = 254 nm. In contrast, after irradiating at λ = 365 nm, the concentration of the MB solution remained around 66.6% in 1 h. It is well-known that the band gap of ZnO is ∼3.37 eV at room temperature. From the equation $\lambda_g = 1240/E_g$ (nm), the absorption edge of ZnO is about 368 nm, only slightly larger than the UV wavelength of 365 nm. In this case, a portion of photons of the UV light with a wavelength of 365 nm cannot be absorbed by the ZnO catalyst and cannot excite electrons from the valence band to the conduction band. On the contrary, UV light with a wavelength of 254 nm can supply enough energy to effectively generate electrons and holes. In other words, the electrons in the valence band of ZnO are much easier to absorb the energy to jump to the conduct band by the excitation from the 254 nm source, which then are transferred to the graphene. The lifetime as well as the concentrations of charges can increases, leading to the enhanced photocatalytic effect.[18,34]

Photocatalytic activities of catalysts with different proportional ratios for the photocatalytic degradation of MB under UV irradiation (wavelength: 254 nm) are shown in Figure 5A. The curve labeled "pure ZnO" was obtained under UV illumination with pure ZnO as a catalyst. The curve labeled "no catalyst" was obtained under UV illumination but without any catalyst. The normalized temporal concentration changes (C/C_0) of MB during the photodegradation are proportional to the normalized maximum absorbance (A/A_0) and derived from the changes in the dye's absorption profile at a given time interval. It can be seen from the figure that there is only little change in the concentration of the solution when the aqueous dye solution is irradiated without any photocatalyst. It is clear from Figure 5A that all the ZnO−GO composites used as photocatalysts exhibited better efficiency in the photodegradation of MB compared to pure ZnO. Under UV light irradiation, more than 93% of the initial dyes were decomposed by ZnO−GO (with ratio of 0.85:0.15) after 1 h. In contrast, nearly 77% of the initial dye still cannot be decomposed in the solution after the same time period for using pure ZnO as a photocatalyst. Figure 5B shows the photocatalytic performance when using ZnO−GO−Pd as a photocatalyst. The apparent rate constant κ_{app} was obtained by line fitting with equation

$$\kappa_{app} = \ln(C_0/C)/t$$

where C_0 is the initial concentration, C is the temporal concentration, and t is the corresponding reaction time.[35] The obtained results revealed that the plots of $\ln(C_0/C)$ versus irradiation time t indicated a good linear relationship ($R^2 \geq 0.959\,27$), which demonstrated that the photocatalytic degradation of MB by ZnO−GO and ZnO−GO−Pd nanocomposites followed the first-order kinetic model. Compared to ZnO−GO, ZnO−GO−Pd works better as photocatalysts on degrading MB in a wider range of weight ratios. Figure 5C shows the photodegradation rates of MB on ZnO−GO photocatalysts and ZnO−GO−Pd photocatalysts with different proportional ratios, which can be used to compare the photocatalytic activities more directly.

It is easy to observe that the optimal proportion ratio of ZnO to GO was 0.85:0.15 for the ZnO−GO system. It is noteworthy that when the amount of GO is below 15 wt %, the photocatalytic activities enhance greatly with the increased loading amount of GO. The sample with 15 wt % GO showed the highest activity (κ_{app} = 0.0394 min^{-1}), which is almost 10

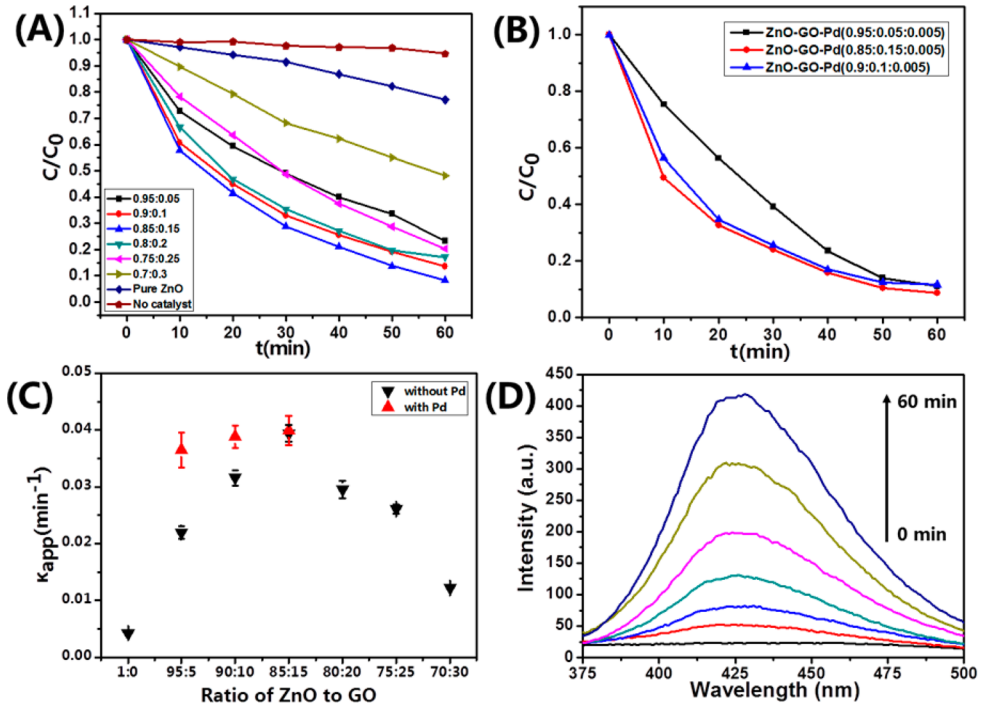

Figure 5. Photodegradation of MB by the as-synthesized (A) ZnO−GO and (B) ZnO−GO−Pd photocatalysts at different weight ratios. (C) Effect of the graphene and Pd NPs loading on the apparent rate constant κ_{app} of MB photodegradation. (D) $^{\bullet}$OH trapping photoluminescence (PL) spectra for ZnO−GO−Pd obtained after irradiation.

times faster than that of ZnO alone. However, when the proportion ratio of GO outnumbers 15 wt %, the photocatalytic activities of as-synthesized photocatalysts decrease with increasing amounts of GO. The decreased activity of the photocatalyst with a weight ratio higher than 15 wt % is attributed to the decreased amount of ZnO, which is the major contributor of electron−hole pairs. After all, GO is an auxiliary material that can enhance the photocatalytic effect but not the active material. Two possible processes might involve in the enhanced catalytic activities of GO in the ZnO−GO system. One is the photogenerated electrons in ZnO might transfer to the GO surface, inhibiting the recombination of electrons and holes. Once photogenerated and separate electrons and holes are caught by the dissolved O_2 and water molecules, respectively, strong oxidizing and catalytic functional groups O_2^- and $^{\bullet}$OH are produced. The higher concentrations of electrons and holes are, the more catalytically active the nanocomposite. The other is that the oxygen functional groups on the GO surface might help to absorb dye molecules to the surface for degradation.

It is also worth noting that there is an obvious enhancement after the introduction of Pd NPs on degrading the dye solution. This phenomenon is observed probably because the Pd NPs located on ZnO−GO are catalytically active and have synergetic effect on photocatalysis. To illustrate this, band diagrams of individual ZnO and Pd are schematically illustrated in Figure 6A. Due to the lower Femi level of ZnO than metal Pd, the energy band of the semiconductor will curve up while they are connected and become a metal-semiconductor Schottky junction under equilibrium, as shown in Figure 6B. When irradiated by UV light (illustrated in Figure 6C as process 1), the electrons of ZnO in the valence band acquire enough energy and jump to the conduction band, leaving the holes behind (process 2). The photogenerated electrons

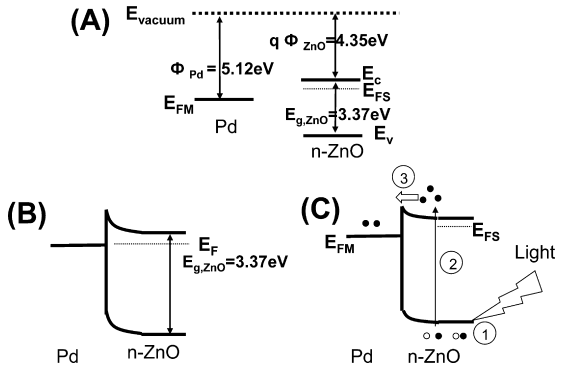

Figure 6. Band diagram analysis of (A) individual ZnO and Pd, (B) ZnO and Pd in contact, and (C) ZnO and Pd in contact under UV light illumination (filled and open circles represent electrons and holes, respectively).

accumulate and then raise the Femi level of ZnO, resulting in electrons transferring from ZnO to metal Pd (process 3). However, the energy barrier of the Schottky junction prevents the electrons in Pd from flowing back to ZnO. This charge separation process effectively reduces the chances of the recombination of newly generated electrons and holes, significantly increasing the lifetime of charges in ZnO−GO−Pd. These accumulated charges with longer lifetimes can produce more quantities of strong oxidizing and catalytic functional groups O_2^- and $^{\bullet}$OH, inducing faster photodegradation.[18] Figure 5D shows the $^{\bullet}$OH-trapping photoluminescence spectra of ZnO−GO−Pd in a terephthalic acid solution at room temperature under UV light irradiation.[36,37] Specifically, a ZnO−GO−Pd (0.85:0.15:0.005) photocatalyst (1 mg) was cast in 50 mL of terephthalic acid solution of 0.2 mmol L^{-1}, and then the solution was stirred in the dark for 30 min. The test for measuring the photodegradation property was

dx.doi.org/10.1021/am405872r | ACS Appl. Mater. Interfaces 2014, 6, 3623−3629

conducted under the UV illumination (wavelength: 254 nm, power 8 W). At given time intervals under UV illumination, 3 mL of the solution was sampled and analyzed by Shimadzu RF-5301PC spectrophotometer. The terephthalic acid was transformed to 2-hydroxy terephthalic acid, which has the photoluminescence emission peak at 426 nm, with the presence of $^{\bullet}$OH. During the reaction process, the photoluminescence emission peak of 2-hydroxy terephthalic acid was gradually enhanced, indicating the continue increase of $^{\bullet}$OH when ZnO−GO−Pd was illuminated with UV light.

In deed, the 254 nm UV light belongs to UV C range and is mostly filtered out by the earth's atmosphere. In practice, people may use this ZnO−GO−Pd catalyst with artificial light sources for dye degradation or apply the knowledge to fabricate other new types of efficient catalysts more suitable for solar spectrum.

4. CONCLUSIONS

With the introduction of GO to ZnO NPs, ZnO−GO photocatalyst is fabricated successfully and it shows significantly enhanced photocatalytic activity for the degradation of MB in the presence of UV light irradiation as compared to pure ZnO. It is worth noting that when the weight ratio of ZnO to GO reaches 0.85:0.15, the as-synthesized ZnO−GO photocatalyst exhibits the optimum photocatalytic efficiency. In addition, with the assistance of noble metal Pd NPs, such ZnO−GO−Pd nanocomposite exhibits generally higher photocatalytic activity in a wider range of weight ratio as compared to ZnO−GO catalysts. GO in ZnO−GO composites does not work as an active photodegradation agent but an auxiliary materials that can depress the recombination of photogenerated electrons and holes. Pd can also form Schottky contact with ZnO in ZnO−GO−Pd nanocomposites, which can also effectively separate photogenerated charges. Our findings provide necessary information to understand the mechanism in the enhanced photocatalytic property in ZnO−GO and ZnO−GO−Pd systems and help to design the next generation of effective and efficient photocatalysts that are believed to have better performance degrading pollutants in water.

AUTHOR INFORMATION

Corresponding Author

*W.J.M. E-mail: wenjiemai@gmail.com.

Author Contributions

$^{\parallel}$These authors contributed equally.

Notes

The authors declare no competing financial interest.

ACKNOWLEDGMENTS

W.J.M. thanks the National Natural Science Foundation of China (Grant No. 51102115, 21376104), the Natural Science Foundation of Guangdong Province, China (Grant No. S2013010012876) for financial support. L.H.D. thanks Jinan University's Scientific Research Creativeness Cultivation Project for Outstanding Undergraduates Recommended for Postgraduate Study.

REFERENCES

(1) Novoselov, K. S.; Schedin, F.; Geim, A. K.; Morozov, S. V.; Hill, E. W.; Blake, P.; Katsnelson, M. I. Detection of individual gas molecules adsorbed on graphene. *Nat. Mater.* **2007**, *6*, 652−655.

(2) Balandin, A. A.; Ghosh, S.; Bao, W. Z.; Calizo, I.; Teweldebrhan, D.; Miao, F.; Lau, C. N. Superior thermal conductivity of single-layer graphene. *Nano Lett.* **2008**, *8*, 902−907.

(3) Hong, B. H.; Kim, K. S.; Zhao, Y.; Jang, H.; Lee, S. Y.; Kim, J. M.; Kim, K. S.; Ahn, J. H.; Kim, P.; Choi, J. Y. Large-scale pattern growth of graphene films for stretchable transparent electrodes. *Nature* **2009**, *457*, 706−710.

(4) Sun, S.; Gao, L.; Liu, Y. Enhanced dye-sensitized solar cell using graphene-TiO_2 photoanode prepared by heterogeneous coagulation. *Appl. Phys. Lett.* **2010**, *96*, 083113−3.

(5) Zhi, L.; Mullen, K. A bottom-up approach from molecular nanographenes to unconventional carbon materials. *J. Mater. Chem.* **2008**, *18*, 1472−1484.

(6) Bolotin, K. I.; Sikes, K. J.; Jiang, Z.; Klima, M.; Fudenberg, G.; Hone, J.; Kim, P.; Stormer, H. L. Ultrahigh electron mobility in suspended graphene. *Solid State Commun.* **2008**, *146*, 351−355.

(7) Nair, R. R.; Blake, P.; Grigorenko, A. N.; Novoselov, K. S.; Booth, T. J.; Stauber, T.; Peres, N. M. R.; Geim, A. K. Fine Structure Constant Defines Visual Transparency of Graphene. *Science* **2008**, *320*, 1308.

(8) Asahi, R.; Morikawa, T.; Ohwaki, T.; Aoki, K.; Taga, Y. Visible-Light Photocatalysis in Nitrogen-Doped Titanium Oxides. *Science* **2001**, *293*, 269−271.

(9) Sakthivel, S.; Neppolian, B.; Shankar, M. V.; Arabindoo, B.; Palanichamy, M.; Murugesan, V. Solar photocatalytic degradation of azo dye: comparison of photocatalytic efficiency of ZnO and TiO_2. *Sol. Energy Mater. Sol. Cells* **2003**, *77*, 65−82.

(10) Chakrabarti, S.; Dutta, B. K. Photocatalytic degradation of model textile dyes in wastewater using ZnO as semiconductor catalyst. *J. Hazard. Mater.* **2004**, *112*, 269−278.

(11) Daneshvar, N.; Salari, D.; Khataee, A. R. Photocatalytic degradation of azo dye acid red 14 in water on ZnO as an alternative catalyst to TiO_2. *J. Photochem. Photobiol., A* **2004**, *162*, 317−322.

(12) Chen, X.; Liu, L.; Yu, P. Y.; Mao, S. S. Increasing Solar Absorption for Photocatalysis with Black Hydrogenated Titanium Dioxide Nanocrystals. *Science* **2011**, *331*, 746−750.

(13) Subramanian, V.; Wolf, E. E.; Kamat, P. V. Catalysis with TiO_2/Gold Nanocomposites. Effect of Metal Particle Size on the Fermi Level Equilibration. *J. Am. Chem. Soc.* **2004**, *126*, 4943−4950.

(14) Young, S. J.; Ji, L. W.; Fang, T. H.; Chang, S. J.; Su, Y. K.; Du, X. L. ZnO ultraviolet photodiodes with Pd contact electrodes. *Acta Mater.* **2007**, *55*, 329−333.

(15) Shu, X.; An, Z.; Wang, L.; He, J. Metal oxide-sensitized TiO_2 and $TiO_{2-x}N_x$ with efficient charge transport conduits. *Chem. Commun.* **2009**, 5901−5903.

(16) Wang, W. W.; Zhu, Y. J.; Yang, L. X. ZnO−SnO_2 Hollow Spheres and Hierarchical Nanosheets: Hydrothermal Preparation, Formation Mechanism, and Photocatalytic Properties. *Adv. Funct. Mater.* **2007**, *17*, 59−64.

(17) Zhao, D.; Sheng, G.; Chen, C.; Wang, X. Enhanced photocatalytic degradation of methylene blue under visible irradiation on graphene@TiO2 dyade structure. *Appl. Catal., B* **2012**, *111−112*, 303−308.

(18) Xu, T.; Zhang, L.; Cheng, H.; Zhu, Y. Significantly enhanced photocatalytic performance of ZnO via graphene hybridization and the mechanism study. *Appl. Catal., B* **2011**, *101*, 382−387.

(19) Li, B.; Cao, H. ZnO@graphene composite with enhanced performance for the removal of dye from water. *J. Mater. Chem.* **2011**, *21*, 3346−3349.

(20) Zhang, J.; Xiong, Z.; Zhao, X. S. Graphene-metal-oxide composites for the degradation of dyes under visible light irradiation. *J. Mater. Chem.* **2011**, *21*, 3634−3640.

(21) Jiang, G.; Lin, Z.; Chen, C.; Zhu, L.; Chang, Q.; Wang, N.; Wei, W.; Tang, H. TiO_2 nanoparticles assembled on graphene oxide nanosheets with high photocatalytic activity for removal of pollutants. *Carbon* **2011**, *49*, 2693−2701.

(22) Chen, C.; Cai, W.; Long, M.; Zhou, B.; Wu, Y.; Wu, D.; Feng, Y. Synthesis of Visible-Light Responsive Graphene Oxide/TiO2 Composites with p/n Heterojunction. *ACS Nano* **2010**, *4*, 6425−6432.

(23) Liu, J.; Bai, H.; Wang, Y.; Liu, Z.; Zhang, X.; Sun, D. D. Self-Assembling TiO_2 Nanorods on Large Graphene Oxide Sheets at a Two-Phase Interface and Their Anti-Recombination in Photocatalytic Applications. *Adv. Funct. Mater.* **2010**, *20*, 4175−4181.
(24) Georgekutty, R.; Seery, M. K.; Pillai, S. C. A Highly Efficient Ag-ZnO Photocatalyst: Synthesis, Properties, and Mechanism. *J. Phys. Chem. C* **2008**, *112*, 13563−13570.
(25) Zheng, Y.; Zheng, L.; Zhan, Y.; Lin, X.; Zheng, Q.; Wei, K. Ag/ZnO Heterostructure Nanocrystals: Synthesis, Characterization, and Photocatalysis. *Inorg. Chem.* **2007**, *46*, 6980−6986.
(26) Liqiang, J.; Baiqi, W.; Baifu, X.; Shudan, L.; Keying, S.; Weimin, C.; Honggang, F. Investigations on the surface modification of ZnO nanoparticle photocatalyst by depositing Pd. *J. Solid State Chem.* **2004**, *177*, 4221−4227.
(27) Hankare, P. P.; Patil, R. P.; Jadhav, A. V.; Garadkar, K. M.; Sasikala, R. Enhanced photocatalytic degradation of methyl red and thymol blue using titania−alumina−zinc ferrite nanocomposite. *Appl. Catal., B* **2011**, *107*, 333−339.
(28) Hummers, W. S.; Offeman, R. E. Preparation of Graphitic Oxide. *J. Am. Chem. Soc.* **1958**, *80*, 1339−1339.
(29) Kovtyukhova, N. I.; Ollivier, P. J.; Martin, B. R.; Mallouk, T. E.; Chizhik, S. A.; Buzaneva, E. V.; Gorchinskiy, A. D. Layer-by-Layer Assembly of Ultrathin Composite Films from Micron-Sized Graphite Oxide Sheets and Polycations. *Chem. Mater.* **1999**, *11*, 771−778.
(30) Geim, A. K.; Novoselov, K. S. The rise of graphene. *Nat. Mater.* **2007**, *6*, 183−91.
(31) Fan, Z.-J.; Kai, W.; Yan, J.; Wei, T.; Zhi, L.-J.; Feng, J.; Ren, Y.-m.; Song, L.-P.; Wei, F. Facile synthesis of graphene nanosheets via Fe reduction of exfoliated graphite oxide. *ACS Nano* **2010**, *5*, 191−198.
(32) Nethravathi, C.; Rajamathi, M. Chemically modified graphene sheets produced by the solvothermal reduction of colloidal dispersions of graphite oxide. *Carbon* **2008**, *46*, 1994−1998.
(33) Szabó, T.; Berkesi, O.; Forgó, P.; Josepovits, K.; Sanakis, Y.; Petridis, D.; Dékány, I. Evolution of surface functional groups in a series of progressively oxidized graphite oxides. *Chem. Mater.* **2006**, *18*, 2740−2749.
(34) Zhang, H.; Lv, X.; Li, Y.; Wang, Y.; Li, J. P25-graphene composite as a high performance photocatalyst. *ACS Nano* **2009**, *4*, 380−386.
(35) Yang, L.-Y.; Dong, S.-Y.; Sun, J.-H.; Feng, J.-L.; Wu, Q.-H.; Sun, S.-P. Microwave-assisted preparation, characterization and photocatalytic properties of a dumbbell-shaped ZnO photocatalyst. *J. Hazard. Mater.* **2010**, *179*, 438−443.
(36) Barreto, J. C.; Smith, G. S.; Strobel, N. H. P.; McQuillin, P. A.; Miller, T. A. Terephthalic acid: A dosimeter for the detection of hydroxyl radicals in vitro. *Life Sci.* **1994**, *56*, 89−96.
(37) Hirakawa, T.; Nosaka, Y. Properties of O_2-and OH formed in TiO_2 Aqueous Suspensions by Photocatalytic Reaction and the Influence of H_2O_2 and Some Ions. *Langmuir* **2002**, *18*, 3247−3254.